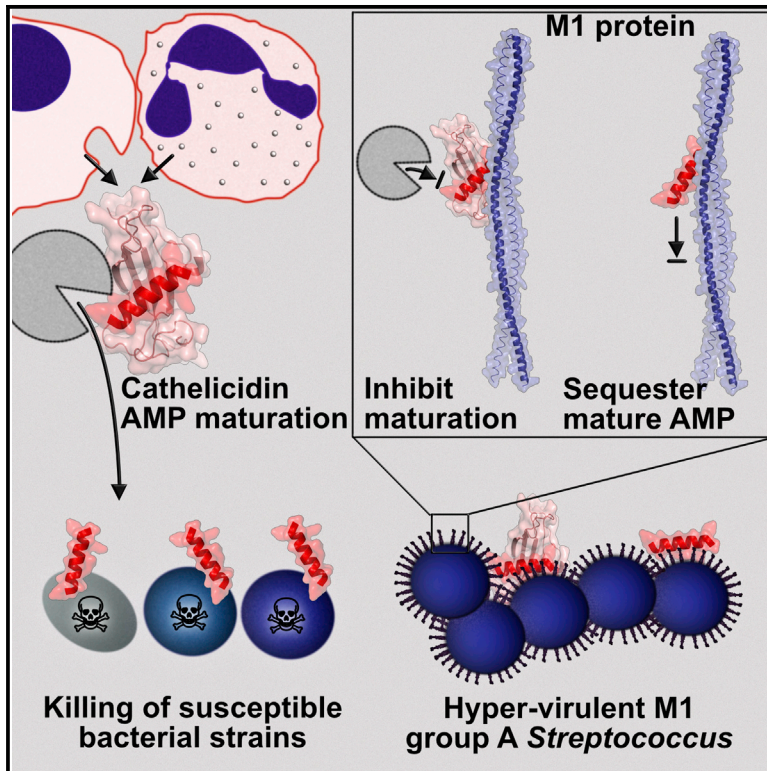


Cell Host & Microbe

Group A Streptococcal M1 Protein Sequesters Cathelicidin to Evade Innate Immune Killing

Graphical Abstract



Authors

Christopher N. LaRock,
Simon Döhrmann, Jordan Todd, ...,
Richard L. Gallo, Partho Ghosh,
Victor Nizet

Correspondence

vnizet@ucsd.edu

In Brief

A globally disseminated clone of hyperinvasive M1T1 group A *Streptococcus* (GAS) causes severe infections, including necrotizing fasciitis. LaRock et al. show that M1T1 GAS circumvents immune defenses mediated by human cathelicidin LL-37 by binding this antimicrobial peptide through the bacterial surface protein M1 and sequestering it in a protein trap.

Highlights

- Hypervirulent M1 group A *Streptococcus* (GAS) resists innate immune clearance
- The surface-expressed GAS M1 protein sequesters human cathelicidin LL-37
- M1 protein sequestration of immature cathelicidin blocks its activation
- The pathogenesis of GAS necrotizing fasciitis requires cathelicidin inhibition



Group A Streptococcal M1 Protein Sequesters Cathelicidin to Evade Innate Immune Killing

Christopher N. LaRock,¹ Simon Döhrmann,¹ Jordan Todd,¹ Ross Corriden,¹ Joshua Olson,¹ Timo Johannsen,^{5,6} Bernd Lepenies,^{5,6,7} Richard L. Gallo,^{1,3} Partho Ghosh,² and Victor Nizet^{1,4,*}

¹Department of Pediatrics

²Department of Chemistry and Biochemistry

³Department of Dermatology

⁴Skaggs School of Pharmacy and Pharmaceutical Sciences

University of California, San Diego, La Jolla, CA 92093, USA

⁵Department of Biomolecular Systems, Max Planck Institute of Colloids and Interfaces, 14476 Potsdam, Germany

⁶Institute of Chemistry and Biochemistry, Department of Biology, Chemistry and Pharmacy, Freie Universität Berlin, 14195 Berlin, Germany

⁷Research Center for Emerging Infections and Zoonoses, University of Veterinary Medicine Hannover, 30559 Hannover, Germany

*Correspondence: vnizet@ucsd.edu

<http://dx.doi.org/10.1016/j.chom.2015.09.004>

SUMMARY

The antimicrobial peptide LL-37 is generated upon proteolytic cleavage of cathelicidin and limits invading pathogens by directly targeting microbial membranes as well as stimulating innate immune cell function. However, some microbes evade LL-37-mediated defense. Notably, group A *Streptococcus* (GAS) strains belonging to the hypervirulent M1T1 serogroup are more resistant to human LL-37 than other GAS serogroups. We show that the GAS surface-associated M1 protein sequesters and neutralizes LL-37 antimicrobial activity through its N-terminal domain. M1 protein also binds the cathelicidin precursor hCAP-18, preventing its proteolytic maturation into antimicrobial forms. Exogenous M1 protein rescues M1-deficient GAS from killing by neutrophils and within neutrophil extracellular traps and neutralizes LL-37 chemotactic properties. M1 also binds murine cathelicidin, and its virulence contribution in a murine model of necrotizing skin infection is largely driven by its ability to neutralize this host defense peptide. Thus, cathelicidin resistance is essential for the pathogenesis of hyperinvasive M1T1 GAS.

INTRODUCTION

Cathelicidins are cationic antimicrobial peptides produced by leukocytes and epithelial cells that provide a critical first line of defense against microbial invasion (Wong et al., 2013; Nizet et al., 2001). Cathelicidin expression is strongly induced during infection and injury (Dorschner et al., 2001), initially as a full-length protein that lacks antimicrobial activity (Zaiou et al., 2003). Neutrophil proteinase-3 and keratinocyte kallikreins process cathelicidin to liberate antimicrobial peptides derived from its carboxyl terminus (Murakami et al., 2004; Sørensen et al., 2001; Yamasaki et al., 2006). Some cathelicidin peptides,

the best characterized being human LL-37, also function as signaling molecules to stimulate inflammation (Yamasaki et al., 2007), production of other antimicrobials (Alalwani et al., 2010), chemotaxis (De Yang et al., 2000), and formation of neutrophil extracellular traps (NETs) (Neumann et al., 2014).

Streptococcus pyogenes (group A *Streptococcus*; GAS) is a leading human pathogen, associated with hundreds of millions of pharyngeal and skin infections yearly (Carapetis et al., 2005). GAS are commonly classified on the basis of the antigenically variable surface M protein, an important virulence factor encoded by the *emm* gene, of which >200 genotypes have been characterized (McMillan et al., 2013). The past several decades have witnessed an increase in severe invasive forms of GAS infection such as necrotizing fasciitis and streptococcal toxic shock syndrome, largely attributable to the rise of a single globally disseminated hyperinvasive M1T1 (*emm1*) clone (Aziz and Kotb, 2008; Walker et al., 2014). The ability of M1T1 GAS to produce serious infections defines an intrinsic resistance to innate immune defenses that normally restrict GAS invasiveness. Indeed, compared to other serotype strains, M1T1 serotype GAS are highly resistant to the cathelicidin-derived peptide LL-37 and to NETs (Lauth et al., 2009), in which cathelicidin is highly abundant. Here, we sought to examine the molecular mechanism underlying the cathelicidin resistance of M1T1 GAS and the extent to which it contributes to the increased virulence of these isolates.

RESULTS

GAS Is Protected by M1 Protein Binding of LL-37

M1T1 GAS lacking M1 protein are more susceptible to killing by human cathelicidin LL-37 (Lauth et al., 2009). M protein is the most abundant protein on the GAS surface (Severin et al., 2007), extending from the bacterial cell surface in the form of hair-like fimbriae (Phillips et al., 1981). One important category of streptococcal antimicrobial peptide resistance mechanisms involves electrostatic repulsion of the cationic peptides away from the bacterial surface (LaRock and Nizet, 2015). However, we found by flow cytometry that M1T1 GAS bound significantly more LL-37 than isogenic $\Delta emm1$ mutant bacteria (Figures 1A

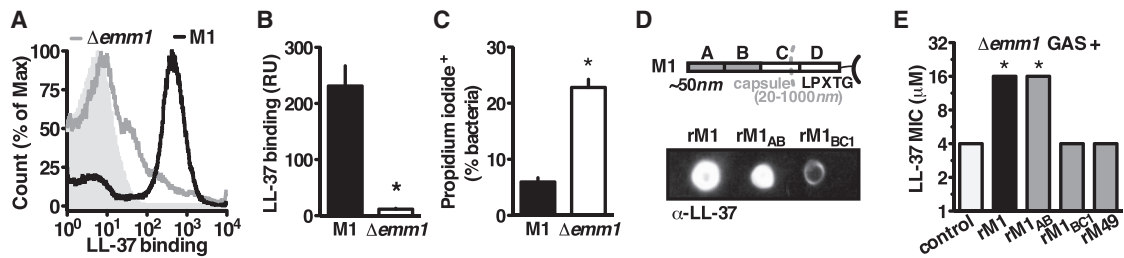


Figure 1. GAS Is Protected by M1 Protein Binding of LL-37

(A–C) Mid-log WT or $\Delta emm1$ M1T1 GAS were incubated with 2 μ M LL-37 and propidium iodide. (A and B) FACS detection of LL-37 on the bacterial surface with anti-LL-37 antibody indicates that $\Delta emm1$ GAS binds significantly less LL-37 than WT GAS. (C) Flow cytometric quantification of cells staining positive for propidium iodide shows significantly more $\Delta emm1$ GAS have disrupted cell walls compared to WT. RU, relative units.

(D) Dot blot of pull-down analysis with His-tagged recombinant M protein and LL-37, detected by western blot with anti-LL-37 antibody.

(E) MIC assay of LL-37-susceptible $\Delta emm1$ GAS with recombinant M protein to increase resistance.

Means \pm SD (n = 3) are shown. *p < 0.05. Figures are representative of at least three independent experiments.

and 1B). Despite binding more cathelicidin, fewer of the M1-expressing GAS were killed as quantified by propidium iodide uptake (Figure 1C). These results indicate that M1 does not repel LL-37, yet still protects GAS from killing by the antimicrobial peptide.

We hypothesized that M1 protein could provide an alternative binding site to entrap LL-37 away from the bacterial membrane, thereby preserving bacterial cell integrity. Through pull-down analysis, we found that recombinant M1 protein directly bound LL-37 (Figure 1D). Further mapping of this interaction using M1-derived fragments revealed that the region most distal to the bacterial surface, carrying the A region and B repeats (M1_{AB}), was sufficient for binding (Figure 1D). The addition of recombinant M1 or M1_{AB} to cultures of $\Delta emm1$ GAS reversed the LL-37 susceptibility phenotype of the mutant (Figure 1E), whereas no protective effect was seen with recombinant M protein from less invasive M49 serotype GAS (Figure 1E). This suggests that the linkage of M1 protein to LL-37 resistance is independent of cell alterations due to M1 deletion but rather derives from direct sequestration of LL-37 by M1 protein.

M1 Binds Immature Cathelicidin to Block Antimicrobial Peptide Generation

To examine whether M1 sequestration of LL-37 is functional in an infection context, we performed pull-down analysis using whole lysates from neutrophils, the major producers of the human defense peptide (Sørensen et al., 2001). Surprisingly, the major cathelicidin form detected was uncleaved hCAP18 (Figure 2A). This was confirmed by flow cytometric analysis, where recombinant hCAP18 bound the GAS surface in an M1-dependent manner (Figures 2B and 2C). Surface plasmon resonance confirmed a high differential affinity of M1 protein to both LL-37 and hCAP-18. Compared to M49 protein, calculated diffusion constant (K_d) values for M1 indicated 53-fold stronger binding to LL-37 (1.18 μ M versus 62.67 μ M) and 10-fold stronger binding to hCAP-18 (0.92 μ M versus 9.07 μ M) (Figure 2D).

In addition to binding LL-37 and hCAP18, M1 also bound the peptides KR-20 and KR-12 (Figure 2E), the most active processed forms of cathelicidin expressed by keratinocytes in human skin (Yamasaki et al., 2006). This activity was not limited to human cathelicidin, as the active murine form, mCRAMP,

was also bound (Figure 2E). Consistent with binding cathelicidin family peptides, M1 protected GAS from killing by KR-20, KR-12, LL-37, and mCRAMP, but not from the similarly charged defensin-family peptides α -defensin-1 (hNP1), β -defensin-1 (hBD1), β -defensin-2 (hBD2), and β -defensin-3 (hBD3) (Figure 2F).

Unprocessed hCAP18 lacked antimicrobial activity (Figure 2F), consistent with previous reports that only the cleavage products are active (Zaiou et al., 2003). Antimicrobial binding and killing are coupled properties of its cationic charge (Lai and Gallo, 2009), so it was surprising that immature cathelicidin interacted with the bacterium without toxicity. M1 protein binding of immature cathelicidin suggested the possibility that the proteolytic maturation of cathelicidin into antimicrobial peptides could be altered. Indeed, M1 inhibited hCAP18 processing by the neutrophil proteinase-3 (PRTN3) (Sørensen et al., 2001) and the keratinocyte kallikrein-5 (KLK5) (Yamasaki et al., 2006) (Figure 2G). M1 did not inhibit PRTN3 or KLK5 processing of another substrate (Figure 2H), indicating that M1 is not acting broadly as a protease inhibitor. Instead, this suggests that hCAP18 is protected from proteolytic activation when complexed with M1, allowing GAS to inhibit the generation of antimicrobial peptides.

Multipronged Innate Immune Cell Subversion by M1 through Cathelicidin Sequestration

M1 protein is reported to promote GAS survival during interactions with neutrophils (Lauth et al., 2009) and macrophages (Hertzén et al., 2010), two of the major producers of cathelicidin (LaRock and Nizet, 2015). We found that wild-type (WT) GAS was more resistant to human neutrophil killing than the $\Delta emm1$ mutant (Figure 3A) and survived better within NETs (Figure 3B). However, the attenuated survival of the $\Delta emm1$ mutant incubated with neutrophils or NETs was reversed by the addition of exogenous recombinant M1 protein (Figures 3A and 3B). In neither instance did the addition of rM1 promote further survival of WT GAS, indicating that the native expression of M1 is sufficient to afford complete protection against neutrophil-expressed cathelicidin. These findings indicate that M1 does not have to be expressed on the bacterial surface to be protective, consistent with the molecular mechanism of cathelicidin sequestration.

To determine whether M1 inhibition of cathelicidin contributes to GAS resistance to macrophage killing, we infected

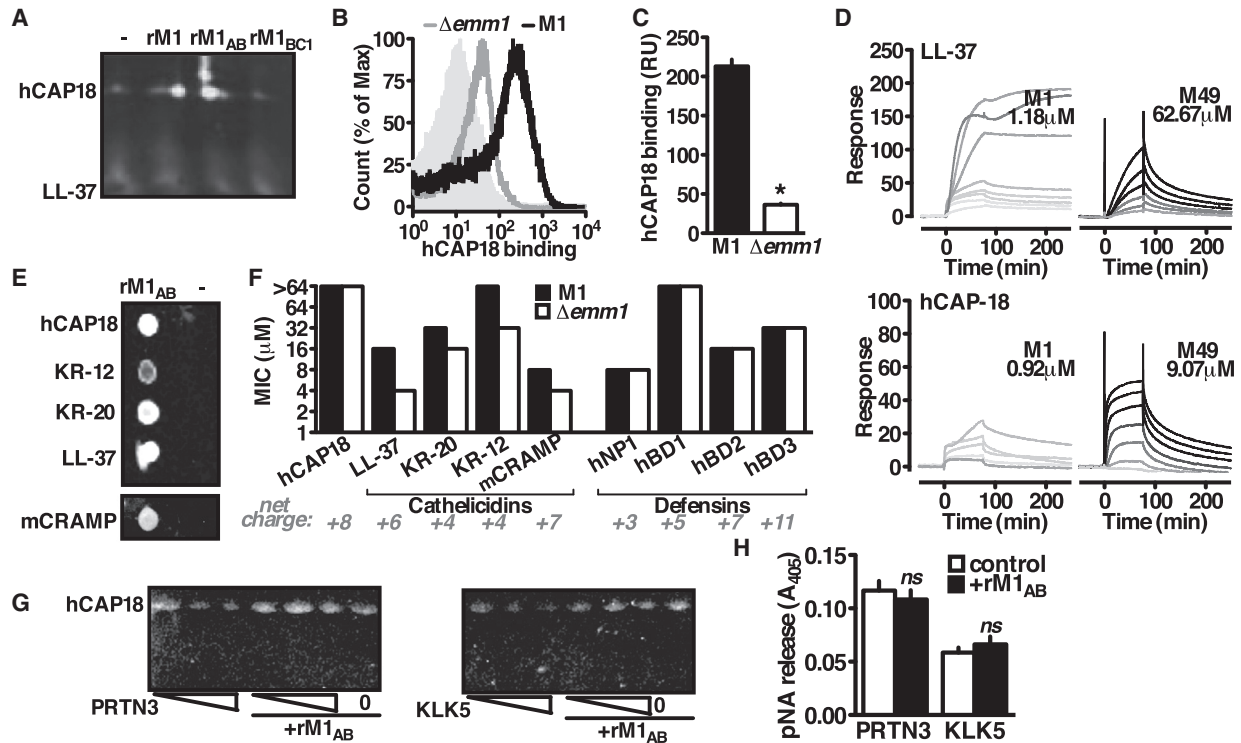


Figure 2. M1 Binds Immature Cathelicidin to Block Antimicrobial Peptide Generation

(A) Interaction between rM1 and cathelicidin from neutrophil lysate by pull-down analysis and western blot using anti-LL-37 antibody. (B and C) In (B), flow cytometric detection of recombinant hCAP18 on the bacterial surface with anti-LL-37 antibody indicates that $\Delta emm1$ GAS binds significantly less hCAP18 than WT GAS, quantified in (C). (D) Representative sensorgrams from surface plasmon resonance analysis of M1 or M49 protein binding to immobilized LL-37 or hCAP18. Gray scale indicates concentration of M protein analyte in 2-fold dilutions starting from 80 μM (black) to 78.125 nM (lightest gray) at 5 μM (M1-LL-37), 80 μM (M49-LL-37), 1.25 μM (M1-hCAP18), or 80 μM (M49-hCAP18). (E) Pull-down analysis with rM1 as bait for full-length (hCAP18) or truncated (LL-37, KR-20, KR-12, mCRAMP) forms as shown by dot blot probed with anti-LL-37 antibody. (F) Resistance of WT and $\Delta emm1$ GAS to full-length cathelicidin and the antimicrobial peptides from the cathelicidin (LL-37, KR-20, KR-12, mCRAMP) and defensin (hNP1, hBD1, hBD2, hBD3) families. (G) Cleavage of recombinant hCAP18 by increasing amounts of PRTN3 or KLK5 (one, two, or five enzymatic units) in the presence or absence of rM1, as visualized by western blot with anti-LL-37 antibody. (H) Enzymatic activity of PRTN3 or KLK5 in the presence of rM1. ns, not significant. Figures are representative of at least three independent experiments.

macrophages derived from WT (C57BL/6) and cathelicidin-deficient (CRAMP^{-/-}) mice. Compared to the WT GAS, the $\Delta emm1$ mutant had markedly attenuated survival in WT macrophages but similar growth in CRAMP^{-/-} macrophages (Figure 3C). In human cells, vitamin D strongly induces cathelicidin expression (Liu et al., 2006). We found that $\Delta emm1$ GAS became hyper-susceptible to killing by human THP-1 macrophages when cathelicidin expression was amplified by vitamin D treatment (Figure 3D). Cathelicidin is also abundantly produced by mast cells and contributed to killing of the cathelicidin-susceptible serotype M49 GAS in the mouse model (Di Nardo et al., 2008). We found that M1 promoted GAS resistance to killing by murine mast cells in a cathelicidin-dependent manner (Figure 3E).

In addition to microbial killing, cathelicidin cleavage products further amplify the innate immune response by stimulating chemotaxis of neutrophils to the foci of infection (De Yang et al., 2000). We tested the effect of M1 protein on LL-37-mediated chemotaxis using a Transwell system. LL-37 and the posi-

tive control N-formyl-Met-Leu-Phe (fMLP) both stimulated robust chemotaxis of neutrophils (Figure 3F). rM1 did not stimulate or inhibit chemotaxis on its own but did inhibit LL-37-mediated migration (Figure 3G). Chemotaxis inhibition by the M1 protein further indicates that interfering with cathelicidin function is a virulence strategy that can promote bacterial survival by several modalities.

GAS Inhibition of Cathelicidin Permits Invasive Infection

Our in vitro analyses suggest that M1 protein binding of cathelicidin could promote GAS innate immune resistance in several manners. To examine the contribution of cathelicidin sequestration by the M1 protein on GAS in vivo, we used a subcutaneous wound infection model with C57BL/6 and CRAMP^{-/-} littermate mice and followed the development of necrotic skin ulcers at the site of GAS inoculation. In WT mice, WT M1 GAS produced larger lesions than the $\Delta emm1$ mutant, consistent with the known virulence role of the M1 protein (Figures 4A and 4B).

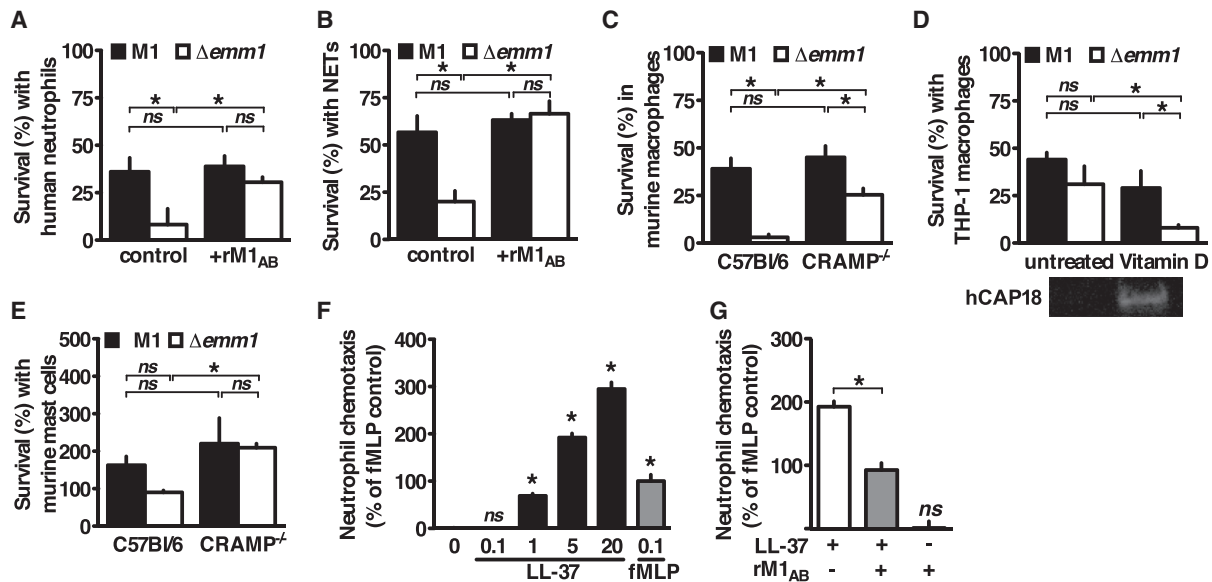


Figure 3. Multipronged Innate Immune Cell Subversion by M1 through Cathelicidin Sequestration

(A and B) Human neutrophils were infected with GAS for 2 hr, (A) untreated, or (B) after 4 hr pretreatment with 25 nM phorbol 12-myristate 13-acetate to induce NET formation.

(C–E) Cells derived from C57BL/6 or CRAMP^{-/-} mice (C and E) or culture (D) were primed with 100 ng/ml lipopolysaccharide (C and E) or 20 nM vitamin D (active 1,25D₃ form) (D) for 18 hr and then infected with WT M1 or $\Delta emm1$ GAS for 2 hr.

(F and G) Human neutrophils were seeded in the upper chamber of a 3- μ m Transwell with LL-37, fMLP, and/or recombinant M1 protein in the lower chamber, and migration was measured by myeloperoxidase activity in the lower chamber after 1 hr.

Means \pm SD (n = 3) are shown. *p < 0.05; ns, not significant. Figures are representative of at least three independent experiments.

Remarkably, in CRAMP-deficient^{-/-} mice, $\Delta emm1$ GAS was able to form lesions of size comparable to WT GAS (Figures 4A and 4B). This reversal of attenuation in CRAMP^{-/-} mice was not seen for $\Delta emm49$ GAS (Figures 4E and 4F), which agrees with the observation that M1, but not M49, binds and inhibits CRAMP. Interestingly, M49 GAS formed larger lesions in CRAMP^{-/-} mice (Figures 4E and 4F), whereas M1 GAS produced similar sized lesions in WT and cathelicidin-deficient animals (Figures 4A and 4B), suggesting that the M1 protein effectively counteracts the cathelicidin contribution to innate defense in this localized GAS infection model.

When bacteria were harvested for colony-forming-unit (CFU) enumeration 72 hr after infection, the $\Delta emm1$ GAS recovered from WT mice were comparable to the initial inoculum, whereas WT M1 GAS had proliferated over one order of magnitude (Figure 4C). Consistent with the lesion size data, in vivo proliferation of $\Delta emm1$ GAS was restored to WT levels in CRAMP^{-/-} mice (Figure 4C). Together, these data suggest that, while M proteins have many virulence functions, cathelicidin inhibition is the major virulence contribution of the M1 protein in this model. Although $\Delta emm49$ was similarly attenuated in WT mice, its growth was not similarly restored in CRAMP^{-/-} mice (Figure 4G). This indicates that the attenuation reversal of $\Delta emm1$ is specifically due to the ability of M1 to inhibit cathelicidin and not a more generalized immune defect of CRAMP^{-/-} mice. Highlighting these differences in another way, the growth index of WT M1 GAS was greater than the isogenic $\Delta emm1$ mutant only in WT mice where cathelicidin is expressed (Figure 4D), whereas M49 contribution to virulence was independent of host cathelicidin expression (Figure 4H).

DISCUSSION

Antimicrobial peptides provide a countermeasure against bacteria that is conserved across all kingdoms of life. Mice lacking cathelicidin antimicrobial peptides are more susceptible to infection (Nizet et al., 2001), and qualitative defects in cathelicidin expression or activity play a role in the increased infection rates of humans with cystic fibrosis (Goldman et al., 1997), morbus Kostmann (Pütsep et al., 2002), and chronic vitamin D deficiency (Liu et al., 2006). Conversely, dysregulated and excessive levels of cathelicidin expression can be damaging to the host and a driver of diseases such as rosacea (Yamasaki et al., 2007), hidradenitis suppurativa (Emelianov et al., 2012), and cigarette-smoke-associated chronic obstructive pulmonary disease (Sun et al., 2014). Cathelicidin expression may be limited because of these proinflammatory liabilities to levels for which resistance by pathogens is possible.

Our results show that one pathogenic bacterial clone, hypervirulent M1T1 GAS, has developed high-level cathelicidin resistance. Indeed, M1 GAS produced equivalent lesions and bacterial loads in WT and CRAMP^{-/-} mice, indicating that it is fully resistant to cathelicidin in vivo, which has provided it a significant virulence benefit. In contrast, M49 GAS has not evolved high-level resistance to cathelicidin. It causes more severe disease in CRAMP^{-/-} mice than WT, as is true for other pathogens tested (Bergman et al., 2006; Chromek et al., 2006; Huang et al., 2007; Kovach et al., 2012; Nizet et al., 2001). Therefore physiological levels of cathelicidin are restrictive for other GAS strains, but M1 protein allows the resistance of hypervirulent M1T1 GAS to levels above those achieved in vivo.

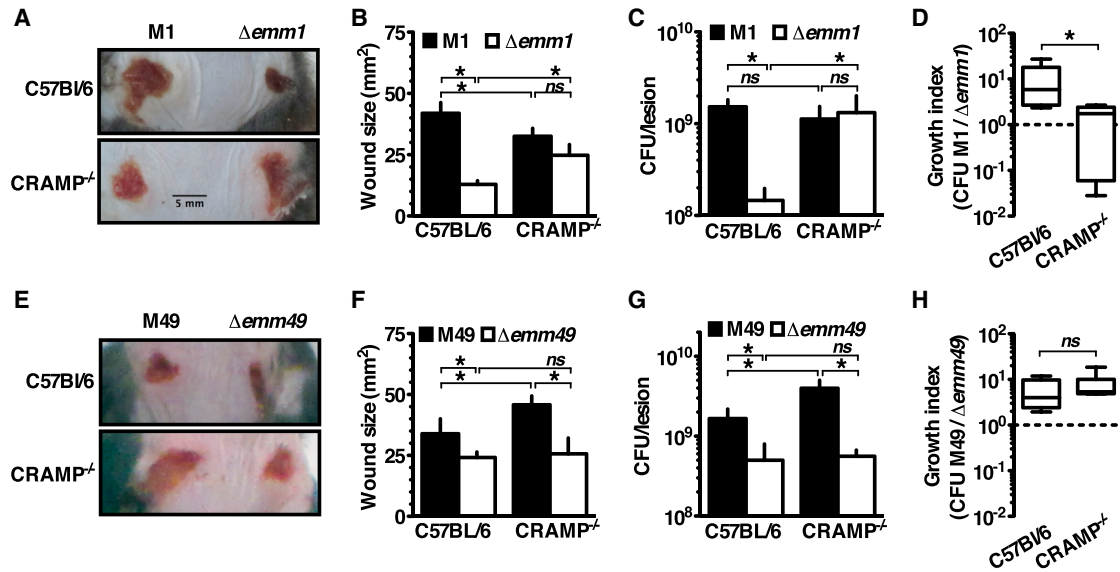


Figure 4. GAS Inhibition of Cathelicidin Permits Invasive Infection

(A–H) Mice were infected subcutaneously with the GAS strains indicated for 72 hr.

(A and E) GAS mutant for M protein ($\Delta emm1$; $\Delta emm49$) formed smaller lesions in cathelicidin-expressing mice (WT, C57BL/6), but the capacity to form lesions was restored for $\Delta emm1$ in CRAMP^{-/-} mice.

(B and F) Average lesion sizes enumerated in (B) and (F) demonstrate that these differences are significant.

(C and G) Lesions were excised and homogenized, and CFUs were enumerated by dilution plating.

(D and H) Growth index, measuring growth of WT bacteria compared to *emm* mutants, showed WT GAS outcompeting mutant bacteria 10-fold, except in CRAMP^{-/-} mice, where M1 and M1 $\Delta emm1$ grew comparably.

Means \pm SD (n = 5) are shown. *p < 0.05; ns, not significant. Figures are representative of at least three independent experiments.

M1 protein provides a multifaceted cathelicidin resistance advantage to GAS. Specifically, M1 directly binds LL-37 and other cathelicidin derivatives. This sequestration is sufficient to double or quadruple the concentration of these peptides required to kill the bacterium. Resistance to these peptides carries over to the interaction of GAS with cathelicidin-expressing immune cells such as macrophages, mast cells, and neutrophils. Moreover, M1 protein also inhibits cathelicidin-induced chemotaxis, further promoting GAS evasion of the immune response.

Interestingly, M1 protein bound the uncleaved storage form of cathelicidin in addition to the mature antimicrobial peptides. However, because uncleaved cathelicidin and its activating proteases can be found extracellularly (Sørensen et al., 1999), this may represent another facet of the antimicrobial evasion strategy of GAS. Cathelicidin bound by M1 protein was no longer cleaved by activating proteases, maintaining it in a non-antimicrobial form. By acting upstream of the activation of cathelicidin, GAS is able to pre-empt bacterial killing. In contrast to this two-pronged mechanism we describe for M1 protein, other pathogens are only known to resist antimicrobial peptides through sequestration, degradation, and masking or altering their cell surface (LaRock and Nizet, 2015). Identification of additional antimicrobial peptide-binding virulence factors may reveal this mechanism to be prevalent, with the microbe agnostic to the cleavage state of cathelicidin. Understanding the molecular mechanisms by which microbial pathogens control cathelicidin may provide targets to sensitize the pathogen to innate immune clearance or, conversely, strategies to co-opt the same catheli-

cidin inhibitors for use in immune diseases such as rosacea, where cathelicidin overexpression is implicated.

EXPERIMENTAL PROCEDURES

Bacterial Culture

GAS strains M1T1 5448 and M49 NZ131 and their isogenic Δemm mutants have been previously described (Lauth et al., 2009). GAS strains were routinely propagated at 37°C on Todd-Hewitt broth (THB, Difco). GAS strains grown overnight at 37°C were diluted 1:40 into THB and grown statically at 37°C to an optical density 600 (OD₆₀₀) of 0.400. Bacteria were washed in PBS and diluted to a multiplicity of infection (MOI) of 10 for in vitro experiments. For minimum inhibitory concentration (MIC) assays, 2 \times 10⁵ bacteria were diluted into serum-free DMEM containing phenol red and 10% THB, and the minimum antimicrobial concentration that prevented growth of bacteria after a 24-hr incubation was noted.

Protein Protocols

Expression and purification of rM1, rM1_{AB}, rM1_{BC1}, and rM49 has been described previously (Lauth et al., 2009; Macheboeuf et al., 2011; McNamara et al., 2008). The cathelicidin peptides LL-37, KR-20, KR-12, and mCRAMP were made by de novo synthesis (Anaspec). The full coding sequence of human cathelicidin hCAP18 was chemically synthesized (GenScript) and inserted into the expression vector pET28a. The protein was expressed using standard protocols and native purified by standard protocols in buffer made of 10 mM imidazole, 0.3 M NaCl, 20 mM Na₂HPO₄ (pH 7.4), using cobalt chelate resin (Thermo Fisher). Pull-downs were performed by fixing 5 μ g recombinant 6xHis-tagged M1 protein onto cobalt chelate resin as bait (Thermo Fisher), incubating with 5 μ g cathelicidin and eluting with 100 mM imidazole, with three washes between each step, with the same buffer at all steps (5 mM imidazole, 100 mM NaCl, 20 mM Tris [pH 7]). Samples were run by SDS-PAGE or dot blotted directly onto polyvinylidene fluoride (PVDF) and immunoblotted for LL-37 or CRAMP (Santa Cruz Biotechnology) with IR-conjugated secondary

antibodies (LI-COR Biosciences), and visualized on an Odyssey infrared scanner (LI-COR Biosciences). Proteolysis assays were carried out using 1 μ g cathelicidin and M protein, with the indicated amount of PRTN3 or KLK5 (VWR), and visualized by western blot; or VLD-pNA or AAPV-pNA (Enzo) was added and hydrolysis monitored by an increase in optical density 405 (OD₄₀₅) (Spectramax).

Binding kinetics were analyzed by surface plasmon resonance using the Biacore T100 (GE Healthcare). A C1 sensor chip was activated with 1-ethyl-3-(3-dimethylaminopropyl)carbodiimide and *N*-hydroxysuccinimide. LL-37 or CAP18 in 10 mM sodium acetate (pH 5.5) was injected at 10 μ l/min for 420 s. Remaining reactive groups were quenched using 1 M ethanolamine. In parallel, a reference flow cell was activated and quenched without ligand immobilization. M proteins in PBS, 0.005% Tween-20, were injected at 30 μ l/min for 75 s. After at least 180 s of dissociation, the chip was regenerated using 10 mM glycine-HCl (pH 1.7). Reference and buffer-only values were subtracted, and kinetic analysis was performed using Biacore Evaluation Software (GE Healthcare). K_d values were calculated using a steady-state affinity model. Each experiment was performed twice with similar results.

Cell Culture

Cell lines were cultured in RPMI (GIBCO) containing 10% fetal bovine serum (GIBCO) at 37°C in 5% CO₂ and seeded at 2 × 10⁵ cells per milliliter. THP-1 cells were originally obtained from the ATCC and treated with phorbol 12-myristate 13-acetate (Sigma) 72 hr pre-infection. Murine macrophages, mast cells, and neutrophils were differentiated by standard protocols from the femur exudates of WT C57BL/6 or isogenic CRAMP^{-/-} mice (Nizet et al., 2001). Human neutrophils were isolated from healthy donors using PolyMorphPrep (Axis-Shield) in accordance with the University of California, San Diego, (UCSD) Human Research Protections Program. For total killing, the cells were lysed with 0.05% Triton X-100 for 10 min before dilution plating for CFUs. In intracellular survival experiments, the media were replaced with RPMI containing 100 μ g/ml gentamicin 30 min before lysis and plating. For NET assays, neutrophils were stimulated with 25 nM phorbol 12-myristate 13-acetate (Sigma) 4 hr pre-infection. For chemotaxis assays, 1 × 10⁶ cells were seeded in the upper chambers of 3- μ m-pore Transwell inserts (Corning Life Sciences), with the indicated concentrations of fMLP (Sigma), LL-37 (Anaspec), and rM1 in RPMI in the lower chambers. Following incubation for 1 hr at 37°C with 5% CO₂, Transwell inserts were removed and cells migrated to the lower chamber were lysed via addition of 0.1% Triton X-100. To quantify chemotaxis, the chromogenic elastase substrate *N*-methoxysuccinyl-Ala-Ala-Pro-Val p-nitroanilide was added to lysate samples (1 mM final); following a 30-min incubation at room temperature, absorbance at 405 nm was measured using a Spectra-Max plate reader (Molecular Devices).

Flow Cytometry

For flow cytometry, samples were prepared by growing GAS using the standard protocol followed by a 30-min incubation with 2 μ M LL-37. Cells were washed, blocked 30 min with 10% BSA (Sigma), probed with anti-LL-37 (Santa Cruz Biotechnology) and Alexa Fluor-dye conjugated secondary antibody (Invitrogen), and run on a FACSCalibur system (BD Biosciences). Bacterial cells were gated according to forward and side scatter and the fluorescence intensity measured for a total of 50,000 bacteria. Negative controls of bacteria untreated by LL-37, primary antibody, or secondary antibody were included, and data were analyzed with FlowJo (Tree Star). Cell permeability was monitored in parallel by staining with 10 μ g/ml propidium iodide.

Animal Experiments

The UCSD Institutional Animal Care and Use Committee approved all use and procedures. Eight- to ten-week-old C57BL/6 and littermate CRAMP^{-/-} mice were infected subcutaneously with 1 × 10⁸ (M1) or 6 × 10⁸ (M49) CFUs in 100 μ l of PBS. Lesions were imaged daily and surface area quantified using ImageJ software. At 72 hr, lesions were excised, homogenized, and dilution plated onto THB plates for enumeration of bacterial CFUs.

Statistical Analysis

Statistical significance (**p* < 0.05) was calculated by unpaired Student's *t* test (GraphPad Prism), unless otherwise indicated. Data are representative of at least three independent experiments.

AUTHOR CONTRIBUTIONS

C.N.L., P.G., and V.N. formulated the original hypothesis, designed the study, and analyzed results. C.N.L., S.D., J.T., T.J., R.C., and J.O. performed experiments. B.L. and R.L.G. provided novel reagents. C.N.L. and V.N. wrote the manuscript, and all authors reviewed the manuscript, data, and conclusions before submission.

ACKNOWLEDGMENTS

We would like to thank the members of the P.G. and V.N. labs for their valuable input and Felix Bröcker for assistance with kinetic analysis. This work was supported in part by a fellowship from the A.P. Giannini Foundation (C.N.L.), the German Academic Exchange Service (DAAD) (S.D.), and NIH grants AI052453 (R.L.G. and V.N.), AI096837 (P.G. and V.N.), and AI077780 (V.N.).

Received: June 3, 2015

Revised: August 6, 2015

Accepted: September 2, 2015

Published: October 14, 2015

REFERENCES

- Alalwani, S.M., Sierigk, J., Herr, C., Pinkenburg, O., Gallo, R., Vogelmeier, C., and Bals, R. (2010). The antimicrobial peptide LL-37 modulates the inflammatory and host defense response of human neutrophils. *Eur. J. Immunol.* **40**, 1118–1126.
- Aziz, R.K., and Kotb, M. (2008). Rise and persistence of global M1T1 clone of *Streptococcus pyogenes*. *Emerg. Infect. Dis.* **14**, 1511–1517.
- Bergman, P., Johansson, L., Wan, H., Jones, A., Gallo, R.L., Gudmundsson, G.H., Hökfelt, T., Jonsson, A.-B., and Agerberth, B. (2006). Induction of the antimicrobial peptide CRAMP in the blood-brain barrier and meninges after meningococcal infection. *Infect. Immun.* **74**, 6982–6991.
- Carapetis, J.R., Steer, A.C., Mulholland, E.K., and Weber, M. (2005). The global burden of group A streptococcal diseases. *Lancet Infect. Dis.* **5**, 685–694.
- Chromek, M., Slamová, Z., Bergman, P., Kovács, L., Podracká, L., Ehrén, I., Hökfelt, T., Gudmundsson, G.H., Gallo, R.L., Agerberth, B., and Brauner, A. (2006). The antimicrobial peptide cathelicidin protects the urinary tract against invasive bacterial infection. *Nat. Med.* **12**, 636–641.
- De Yang, Q., Chen, A.P., Schmidt, G.M., Anderson, J.M., Wang, J., Wooters, J., Oppenheim, and Chertov, O. (2000). LL-37, the neutrophil granule- and epithelial cell-derived cathelicidin, utilizes formyl peptide receptor-like 1 (FPRL1) as a receptor to chemoattract human peripheral blood neutrophils, monocytes, and T cells. *J. Exp. Med.* **192**, 1069–1074.
- Di Nardo, A., Yamasaki, K., Dorschner, R.A., Lai, Y., and Gallo, R.L. (2008). Mast cell cathelicidin antimicrobial peptide prevents invasive group A *Streptococcus* infection of the skin. *J. Immunol.* **180**, 7565–7573.
- Dorschner, R.A., Pestonjans, V.K., Tamakuwala, S., Ohtake, T., Rudisill, J., Nizet, V., Agerberth, B., Gudmundsson, G.H., and Gallo, R.L. (2001). Cutaneous injury induces the release of cathelicidin anti-microbial peptides active against group A *Streptococcus*. *J. Invest. Dermatol.* **117**, 91–97.
- Emelianov, V.U., Bechara, F.G., Gläser, R., Langan, E.A., Taungjaruwinai, W.M., Schröder, J.M., Meyer, K.C., and Paus, R. (2012). Immunohistological pointers to a possible role for excessive cathelicidin (LL-37) expression by apocrine sweat glands in the pathogenesis of hidradenitis suppurativa/acne inversa. *Br. J. Dermatol.* **166**, 1023–1034.
- Goldman, M.J., Anderson, G.M., Stolzenberg, E.D., Kari, U.P., Zasloff, M., and Wilson, J.M. (1997). Human β -defensin-1 is a salt-sensitive antibiotic in lung that is inactivated in cystic fibrosis. *Cell* **88**, 553–560.
- Hertzén, E., Johansson, L., Wallin, R., Schmidt, H., Kroll, M., Rehn, A.P., Kotb, M., Mörgelin, M., and Norrby-Teglund, A. (2010). M1 protein-dependent intracellular trafficking promotes persistence and replication of *Streptococcus pyogenes* in macrophages. *J. Innate Immun.* **2**, 534–545.
- Huang, L.C., Reins, R.Y., Gallo, R.L., and McDermott, A.M. (2007). Cathelicidin-deficient (Cnlp^{-/-}) mice show increased susceptibility to

- Pseudomonas aeruginosa* keratitis. Invest. Ophthalmol. Vis. Sci. 48, 4498–4508.
- Kovach, M.A., Ballinger, M.N., Newstead, M.W., Zeng, X., Bhan, U., Yu, F.S., Moore, B.B., Gallo, R.L., and Standiford, T.J. (2012). Cathelicidin-related antimicrobial peptide is required for effective lung mucosal immunity in Gram-negative bacterial pneumonia. J. Immunol. 189, 304–311.
- Lai, Y., and Gallo, R.L. (2009). AMPed up immunity: how antimicrobial peptides have multiple roles in immune defense. Trends Immunol. 30, 131–141.
- LaRock, C.N., and Nizet, V. (2015). Cationic antimicrobial peptide resistance mechanisms of streptococcal pathogens. Biochim. Biophys. Acta. Published online February 17, 2015. <http://dx.doi.org/10.1016/j.bbame.2015.02.010>.
- Lauth, X., von Köckritz-Blickwede, M., McNamara, C.W., Myskowski, S., Zinkernagel, A.S., Beall, B., Ghosh, P., Gallo, R.L., and Nizet, V. (2009). M1 protein allows Group A streptococcal survival in phagocyte extracellular traps through cathelicidin inhibition. J. Innate Immun. 1, 202–214.
- Liu, P.T., Stenger, S., Li, H., Wenzel, L., Tan, B.H., Krutzik, S.R., Ochoa, M.T., Schaubert, J., Wu, K., Meinken, C., et al. (2006). Toll-like receptor triggering of a vitamin D-mediated human antimicrobial response. Science 311, 1770–1773.
- Macheboeuf, P., Buffalo, C., Fu, C.Y., Zinkernagel, A.S., Cole, J.N., Johnson, J.E., Nizet, V., and Ghosh, P. (2011). Streptococcal M1 protein constructs a pathological host fibrinogen network. Nature 472, 64–68.
- McMillan, D.J., Drèze, P.A., Vu, T., Bessen, D.E., Guglielmini, J., Steer, A.C., Carapetis, J.R., Van Melder, L., Sriprakash, K.S., and Smeesters, P.R. (2013). Updated model of group A *Streptococcus* M proteins based on a comprehensive worldwide study. Clin. Microbiol. Infect. 19, E222–E229.
- McNamara, C., Zinkernagel, A.S., Macheboeuf, P., Cunningham, M.W., Nizet, V., and Ghosh, P. (2008). Coiled-coil irregularities and instabilities in group A *Streptococcus* M1 are required for virulence. Science 319, 1405–1408.
- Murakami, M., Lopez-Garcia, B., Braff, M., Dorschner, R.A., and Gallo, R.L. (2004). Postsecretory processing generates multiple cathelicidins for enhanced topical antimicrobial defense. J. Immunol. 172, 3070–3077.
- Neumann, A., Berends, E.T., Nerlich, A., Molhoek, E.M., Gallo, R.L., Meerloo, T., Nizet, V., Naim, H.Y., and von Köckritz-Blickwede, M. (2014). The antimicrobial peptide LL-37 facilitates the formation of neutrophil extracellular traps. Biochem. J. 464, 3–11.
- Nizet, V., Ohtake, T., Lauth, X., Trowbridge, J., Rudisill, J., Dorschner, R.A., Pestonjamas, V., Piraino, J., Huttner, K., and Gallo, R.L. (2001). Innate antimicrobial peptide protects the skin from invasive bacterial infection. Nature 414, 454–457.
- Phillips, G.N., Jr., Flicker, P.F., Cohen, C., Manjula, B.N., and Fischetti, V.A. (1981). Streptococcal M protein: α -helical coiled-coil structure and arrangement on the cell surface. Proc. Natl. Acad. Sci. USA 78, 4689–4693.
- Pütsep, K., Carlsson, G., Boman, H.G., and Andersson, M. (2002). Deficiency of antibacterial peptides in patients with morbus Kostmann: an observation study. Lancet 360, 1144–1149.
- Severin, A., Nickbarg, E., Wooters, J., Quazi, S.A., Matsuka, Y.V., Murphy, E., Moutsatsos, I.K., Zagursky, R.J., and Olmsted, S.B. (2007). Proteomic analysis and identification of *Streptococcus pyogenes* surface-associated proteins. J. Bacteriol. 189, 1514–1522.
- Sørensen, O., Bratt, T., Johnsen, A.H., Madsen, M.T., and Borregaard, N. (1999). The human antibacterial cathelicidin, hCAP-18, is bound to lipoproteins in plasma. J. Biol. Chem. 274, 22445–22451.
- Sørensen, O.E., Follin, P., Johnsen, A.H., Calafat, J., Tjabringa, G.S., Hiemstra, P.S., and Borregaard, N. (2001). Human cathelicidin, hCAP-18, is processed to the antimicrobial peptide LL-37 by extracellular cleavage with proteinase 3. Blood 97, 3951–3959.
- Sun, C., Zhu, M., Yang, Z., Pan, X., Zhang, Y., Wang, Q., and Xiao, W. (2014). LL-37 secreted by epithelium promotes fibroblast collagen production: a potential mechanism of small airway remodeling in chronic obstructive pulmonary disease. Lab. Invest. 94, 991–1002.
- Walker, M.J., Barnett, T.C., McArthur, J.D., Cole, J.N., Gillen, C.M., Henningham, A., Sriprakash, K.S., Sanderson-Smith, M.L., and Nizet, V. (2014). Disease manifestations and pathogenic mechanisms of group A *Streptococcus*. Clin. Microbiol. Rev. 27, 264–301.
- Wong, J.H., Ye, X.J., and Ng, T.B. (2013). Cathelicidins: peptides with antimicrobial, immunomodulatory, anti-inflammatory, angiogenic, anticancer and pro-cancer activities. Curr. Protein Pept. Sci. 14, 504–514.
- Yamasaki, K., Schaubert, J., Coda, A., Lin, H., Dorschner, R.A., Schechter, N.M., Bonnart, C., Descargues, P., Hovnanian, A., and Gallo, R.L. (2006). Kallikrein-mediated proteolysis regulates the antimicrobial effects of cathelicidins in skin. FASEB J. 20, 2068–2080.
- Yamasaki, K., Di Nardo, A., Bardan, A., Murakami, M., Ohtake, T., Coda, A., Dorschner, R.A., Bonnart, C., Descargues, P., Hovnanian, A., et al. (2007). Increased serine protease activity and cathelicidin promotes skin inflammation in rosacea. Nat. Med. 13, 975–980.
- Zaiou, M., Nizet, V., and Gallo, R.L. (2003). Antimicrobial and protease inhibitory functions of the human cathelicidin (hCAP18/LL-37) prosequence. J. Invest. Dermatol. 120, 810–816.